

Angle-resolved critical transport-current density of $\text{YBa}_2\text{Cu}_3\text{O}_{7-\delta}$ thin films and $\text{YBa}_2\text{Cu}_3\text{O}_{7-\delta}/\text{PrBa}_2\text{Cu}_3\text{O}_{7-\delta}$ superlattices containing columnar defects of various orientations

B. Holzappel

Physikalisches Institut III, Universität Erlangen-Nürnberg, Erwin-Rommel-Strasse 1, W-8520 Erlangen, Germany and Siemens AG, Research Laboratories, P.O. Box 3220, W-8520 Erlangen, Germany

G. Kreiselmeyer, M. Kraus, and G. Saemann-Ischenko

Physikalisches Institut III, Universität Erlangen-Nürnberg, Erwin-Rommel-Strasse 1, W-8520 Erlangen, Germany

S. Bouffard

Centre Interdisciplinaire de Recherches avec les Ions Lourds, B.P. 5193, F-14040 Caen CEDEX, France

S. Klaumünzer

Hahn-Meitner-Institut, Glienicker Strasse 100, W-1000 Berlin, Germany

L. Schultz

Siemens AG, Research Laboratories, P.O. Box 3220, W-8520 Erlangen, Germany

(Received 4 December 1992)

Epitaxial $\text{YBa}_2\text{Cu}_3\text{O}_{7-\delta}$ thin films irradiated with swift heavy ions under different directions showed a strongly changed angular dependence of the critical current density $J_c(B, T, \vartheta)$ in the mixed state. Additional peaks, which dominate the angular dependence of J_c , appear at angles where the magnetic field is parallel to the irradiation direction, due to the strong pinning of the introduced linear defects. Irradiated $\text{YBa}_2\text{Cu}_3\text{O}_{7-\delta}/\text{PrBa}_2\text{Cu}_3\text{O}_{7-\delta}$ superlattices, however, reveal no additional J_c peaks but an isotropic J_c enhancement in a wide angular range. This contrary behavior could be explained by flux lines of different dimensionality.

The crystal structure of the high- T_c superconductors, where the superconducting CuO planes are separated from each other by distances larger than the coherence length in c direction ξ_c , leads to a more or less $(2+\epsilon)$ -dimensional superconducting behavior, depending on the crystal structure of each family. In this sense, $\text{YBa}_2\text{Cu}_3\text{O}_{7-\delta}$ (YBCO) is a rather three-dimensional (3D) anisotropic superconductor with an anisotropy parameter $\Lambda = \xi_{ab}/\xi_c \approx 5$, whereas $\text{Bi}_2\text{Sr}_2\text{CaCu}_2\text{O}_8$ (BSCCO) ($\Lambda \approx 60$) and the Tl system ($\Lambda \approx 100$) are nearly 2D systems with only small Josephson coupling between the CuO planes.¹ This reduced dimensionality has strong implications on the anisotropy of the superconducting properties and on structure and dynamics of the flux lines (FLs) penetrating the superconductor in the mixed state. The angular dependence of the critical current density $J_c(B, T, \vartheta)$ of YBCO is, e.g., dominated by strong intrinsic pinning due to the reduced order parameter between the superconducting CuO planes²⁻⁴ and the 2D BSCCO system results in an extremely high, temperature- and field-dependent anisotropy ratio of the critical current density $J_c^{B\parallel c}/J_c^{B\perp c}$ because of the magnetic transparency in the $B \perp c$ direction.^{5,6} For YBCO the FLs are rather conventional Abrikosov vortices, whereas for the 2D BSCCO or Tl systems the FLs are strings of 2D point vortices or "pancakes," which are only weakly coupled.^{7,8} This reduced dimensionality of the flux line lattices has also strong implications on

the pinning behavior of columnar defects. The strong pinning activity of columnar defects induced by heavy ion irradiation was shown by measurements of transport properties⁹ and magnetization,¹⁰⁻¹⁴ for both the YBCO and the BSCCO system. TEM investigations^{15,16} demonstrated that the irradiation of YBCO or BSCCO with high-energy heavy ions results, due to the high value of the electronic energy loss of the ions inside the ceramic superconductor, in the formation of linear tubes along the ion linear path, consisting of amorphous or at least strongly disordered material.¹⁷ Therefore, by fixing the irradiation direction relative to the crystal axes one also determines the orientation of the linear defects. For YBCO it was demonstrated that these linear defects show a very selective pinning,¹⁰ being maximal if the applied magnetic field is parallel to the linear defects. BSCCO showed no such effect of a selective pinning¹³ due to the reduced dimensionality of this system. An elegant method to modify the dimensionality of the YBCO system is the preparation of $\text{YBa}_2\text{Cu}_3\text{O}_{7-\delta}/\text{PrBa}_2\text{Cu}_3\text{O}_{7-\delta}$ (YBCO/PBCO) superlattices.¹⁸ According to the number of non-superconducting $\text{PrBa}_2\text{Cu}_3\text{O}_{7-\delta}$ (PBCO) unit cells introduced and the modulation wavelength of the superstructure, one can vary the coupling between the YBCO layers in a broad range. Consequently, also the FL structure should be modifiable in the YBCO system by preparing these superlattices. To test the dimensionality of the FLs and the exact angle dependency of

the selective pinning of linear defects, we studied in this work the effect of columnar defects on the critical current density anisotropy $J_c(B, T, \vartheta)$ of YBCO thin films and YBCO/PBCO superlattices.

Epitaxial YBCO thin films and YBCO/PBCO superlattices were prepared using an excimer laser deposition arrangement, described in detail elsewhere.^{19,20} In general, we used YBCO thin films with a typical thickness of 150 nm and superlattices consisting of 3 unit cells YBCO and variable PBCO layer thicknesses varying from 3 to 20 unit cells [e.g. (10PBCO/3YBCO) \times 12 means a 12 period superlattice, each period consisting of 10 unit cells PBCO and 3 unit cells YBCO]. The samples were patterned by standard photolithography combined with ethylenediamine tetra-acetic acid wet etching into bridges for conventional four-probe transport measurements, typically 20 μ m wide and up to 2 mm long. To generate linear defects, the samples were irradiated by 770 MeV ^{208}Pb ions at the Grand Accélérateur National d'Ions Lourds (Caen), or by 340 MeV ^{126}Xe ions at the Hahn-Meitner-Institute (Berlin). The electronic energy loss of both ions ($S_e^{(770 \text{ MeV Pb})} \approx 3.9 \text{ keV}/\text{\AA}$, $S_e^{(340 \text{ MeV Xe})} \approx 2.9 \text{ keV}/\text{\AA}$) exceeds the threshold of 2 keV/ \AA , where the formation of continuous columnar defects takes place along the trajectory of the ions.²¹ The total energy loss of the ions leads to an implantation depth of 20 μ m, therefore no ion implantation occurs inside the superconducting layers. High-resolution TEM investigations show that these defects consist of amorphous tubes with diameters of $d \approx 50 \text{ \AA}$ (Xe) or $d \approx 80 \text{ \AA}$ (Pb), penetrating the thin film over its total thickness. The samples were irradiated under various angles $\varphi = 0^\circ, 30^\circ, \text{ or } 60^\circ$, with respect to the c -axis of the YBCO lattice (and always perpendicular to the patterned bridge). The fluence of the irradiation was kept constant at $8.0 \times 10^{10} \text{ ions}/\text{cm}^2$ for all samples, corresponding to a dose equivalent field of 1.6 T. This fluence was chosen to achieve a significant irradiation effect in the pinning behavior of the sample, but without any serious degradation of T_c . At the fluence chosen the T_c reduction was less than 1 K. The anisotropy of the critical current density $J_c(B, T, \vartheta)$ was measured using a rotatable refrigerator cooling stage which is placed in

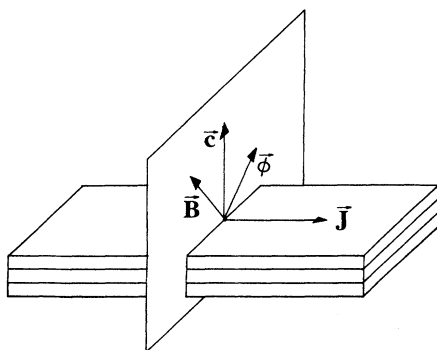


FIG. 1. Schematic representation of the irradiation and measurement directions. [c : c axis of the YBCO thin films; J : current flow direction; ϕ : irradiation direction; B : magnetic field direction; $\vartheta = \langle c, B \rangle$ and $\varphi = \langle c, \phi \rangle$]. J is always perpendicular to B and c .

a normal-conducting split coil magnet with a maximum field strength of 2 T. Rotation of the refrigerator is performed by a computer-controlled stepping motor with a relative angle resolution below 0.01° . J_c was determined using standard four-probe transport measurements with a voltage criterion of $1 \mu\text{V}$. The current direction was always perpendicular to the magnetic-field direction, which rotates in a plane, defined by the c axis of the film and the irradiation direction, as shown in Fig. 1. The irradiation angle φ and the magnetic-field direction ϑ are defined relative to the c axes of the YBCO films, i.e., the normal of the substrate surface. If the magnetic-field direction ϑ equals the irradiation direction φ or $\varphi+180^\circ$, the magnetic field points exactly in the direction of the irradiation-induced amorphous tubes. Figure 2 shows the angular dependence of the critical current density $J_c(B, T, \vartheta)$ of a YBCO thin film before and after irradiation with 770 MeV ^{208}Pb ions. To ensure strong pinning by the columnar defects, a measurement field below the dose equivalent field was chosen. Before the irradiation, $J_c(B, T, \vartheta)$ shows the well-known structure with J_c peaks arising from intrinsic pinning.^{2,3} A common feature of the two intrinsic pinning peaks, observed in most of the anisotropy measurements of YBCO films at higher temperatures, are their different heights due to the differences in the pinning behavior of the film substrate and the film vacuum interface.³ After irradiation at an angle of $\varphi = 60^\circ$, the sample shows a drastically different J_c anisotropy. The intrinsic pinning peaks are reduced by the irradiation, but their relative height ratio remains unchanged. The main difference, however, is the occurrence of two additional peaks in the J_c anisotropy. These two new peaks occur for B exactly at the angle that corresponds to the direction of the introduced linear defects. The absolute heights of these J_c -peaks are comparable to those caused by the intrinsic pinning before the irradiation, indicating that the pinning strength of the artificially introduced defects is comparable to the intrinsic pinning. Due to the fact that the intrinsic pinning peaks

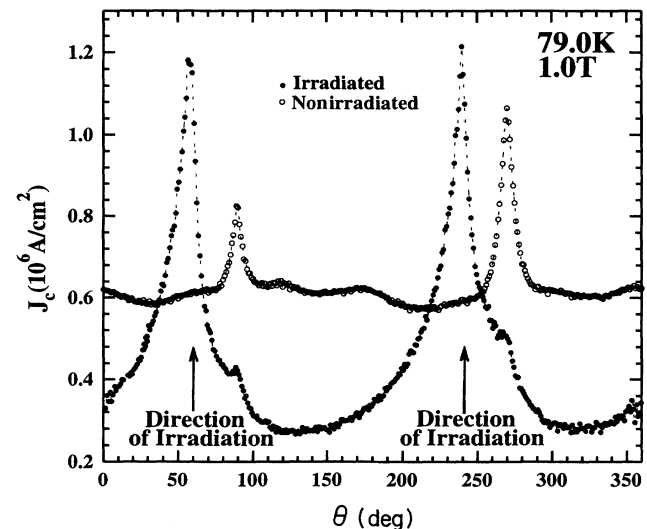


FIG. 2. $J_c(B, T, \vartheta)$ of a YBCO thin film before and after irradiation with 770 MeV ^{208}Pb ions (irradiation direction $\varphi = 60^\circ$, irradiation fluence $8.0 \times 10^{10} \text{ ions}/\text{cm}^2$).

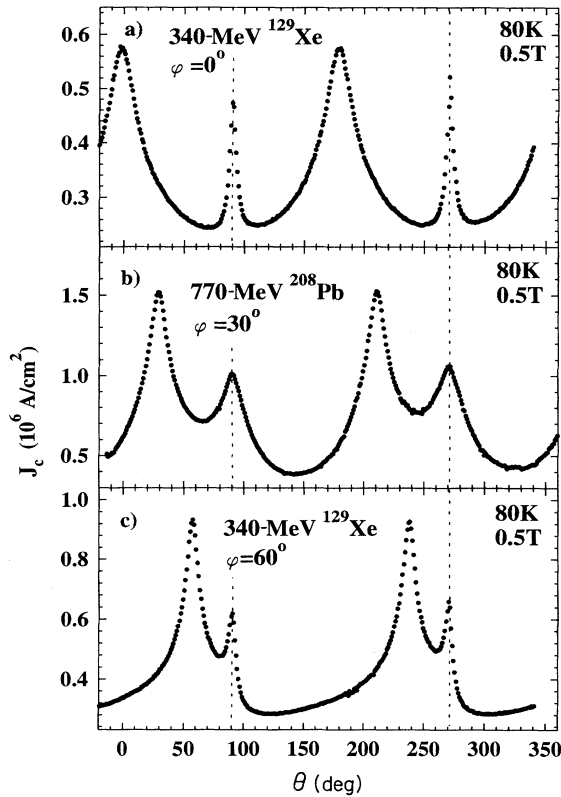


FIG. 3. $J_c(B, T, \vartheta)$ of YBCO thin films after irradiation with 340 MeV ^{129}Xe or 770 MeV ^{208}Pb ions [irradiation direction in Fig. 3(a) : $\varphi = 0^\circ$; Fig. 3(b) : $\varphi = 30^\circ$; Fig. 3(c) : $\varphi = 60^\circ$].

were reduced by the irradiation, the pinning of the linear defects dominates the critical current anisotropy of YBCO. This is the case also for samples irradiated by 340 MeV ^{126}Xe ions and miscellaneous irradiation directions, as shown in Fig. 3. The appearance of additional peaks in the J_c anisotropy of irradiated YBCO thin films can only be explained, if one assumes the presence of 3D rather rigid FLs, which are pinned coherently by the linear defects over distances significantly larger than the intrinsic CuO layer spacing if the magnetic field is parallel to them.

To separate the pinning behavior of the introduced

linear defects from the intrinsic pinning, we measured the magnetic-field dependence of the critical current density $J_c(B)$ for fixed magnetic field directions $\vartheta = \varphi$ and $\vartheta = 180^\circ - \varphi$, i.e., for the magnetic field aligned and misaligned (symmetrical to the intrinsic pinning) to the linear defects. Figure 4(a) shows these measurements for the YBCO film of Fig. 2. For the magnetic-field direction $\vartheta = 180^\circ - \varphi = 120^\circ$ the usual $J_c(B)$ behavior could be observed, whereas for $\vartheta = \varphi = 60^\circ$ the critical current density is enhanced in a broad field range. The difference $\Delta J_c(B) = J_c^{\vartheta=\varphi} - J_c^{\vartheta=180^\circ-\varphi}$, which reflects the contribution of the linear defects to the pinning behavior is shown in Fig. 4(b). The critical current difference has a maximum at a magnetic field of 0.6 T, whereas the volume pinning force $F_p = B\Delta J_c$ gets maximal close to the dose equivalent field of 1.6 T because of matching between the FL spacing and the mean linear defect distance. Due to the equality of the F_p maximum and the equivalent dose field each linear defect pins only one FL.

For the YBCO/PBCO superlattices, the situation is quite different. Figure 5 shows the J_c anisotropy of a $(3\text{PBCO}/3\text{YBCO}) \times 25$ superlattice before and after irradiation with 770 MeV ^{208}Pb ions (irradiation angle $\varphi = 30^\circ$, external field $B_a = 1.0$ T, $T = 70$ K). Before the irradiation the sample shows the well-known $J_c(\vartheta)$ curve which is very similar to the $J_c(\vartheta)$ behavior of the highly anisotropic BSCCO system.⁶ Due to the magnetic transparency in the $B \perp c$ direction, resulting from the introduced PBCO layers, $J_c(B, T, \vartheta)$ follows the equation $J_c(B, T, \vartheta) = J_c(B = B_{\parallel} = B_a \cos(\vartheta), T, \vartheta = 0^\circ)$.²² After the irradiation, the intrinsic J_c peaks are reduced, similar to the YBCO thin film. In contrast to YBCO there are no additional J_c peaks detectable, but a strong J_c enhancement by a factor of 5 could be observed, which is within a wide-angle range completely isotropic, regardless of the particular irradiation direction chosen. This behavior results from a changed FL structure due to the presence of the PBCO layers inside the superlattice, which decouple adjacent YBCO layers. Therefore a FL consists of a number (equivalent to the superlattice period number) of very short (equivalent to the YBCO single layer thickness) FL parts which depin independent from each other and, because of the small YBCO layer thickness (≈ 36 Å), show a nearly 2D behavior comparable to the point vortices in the BSCCO system.²³ The pinning of a FL

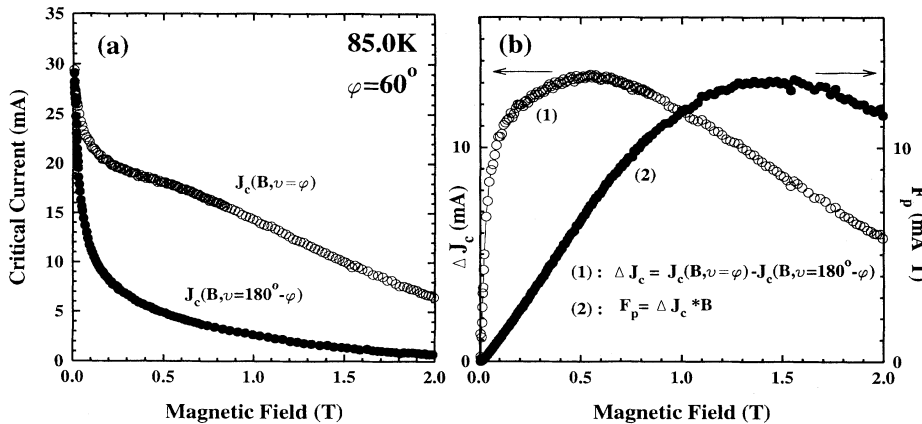


FIG. 4. (a) $J_c(B)$ with the magnetic field aligned ($\vartheta = \varphi$) and misaligned (symmetrical to the intrinsic pinning peak : $\vartheta = 180^\circ - \varphi$) to the linear defects. (b) $\Delta J_c(B) = J_c^{\vartheta=\varphi} - J_c^{\vartheta=180^\circ-\varphi}$ and the volume pinning force $F_p = B\Delta J_c$.

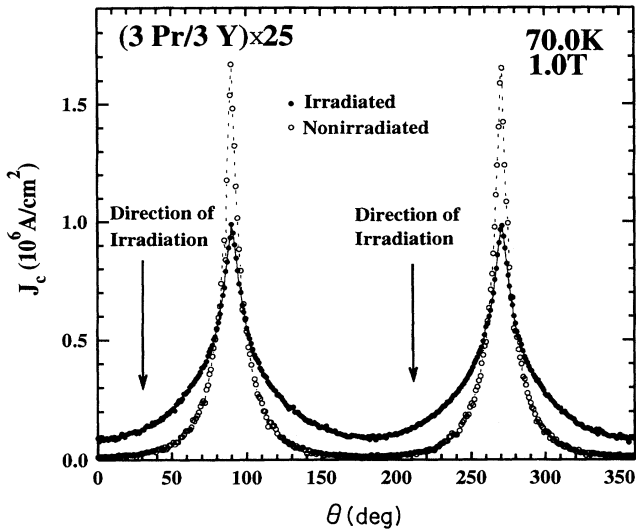


FIG. 5. $J_c(B, T, \vartheta)$ of a $(3\text{PBCO}/3\text{YBCO})\times 25$ superlattice ($T_c^{\text{zero}} = 84\text{ K}$) before and after irradiation with $770\text{ MeV }^{208}\text{Pb}$ ions (irradiation direction $\varphi = 30^\circ$).

by a columnar defect is then reduced to an individual pinning of these pancakelike FL parts by small disks of the linear defect of comparable dimension ($\varnothing \approx 80\text{ \AA}$, $d \approx 36\text{ \AA}$), resulting in the observed independence of the

J_c enhancement on the relative orientation between the magnetic field and the linear defect.

In summary, we present angle-resolved J_c measurements of YBCO thin films and YBCO/PBCO superlattices containing linear defects. For YBCO the coherent pinning of the FLs by the linear defects result in J_c peaks, which appear exactly at the irradiation direction and dominate the intrinsic J_c anisotropy. For the irradiated YBCO/PBCO superlattices, however, we observe an isotropic J_c enhancement due to a decoupled FL structure. These measurements obviously show the coherent pinning capability of columnar defects in YBCO and the strong influence of the FL lattice dimensionality on this pinning behavior.

The authors would like to thank Th. Amrein, A. Thust, B. Kabius (FZ Jülich), and R. Scholz (MPI für Mikrostrukturphysik, Halle) for TEM investigations of irradiated samples, and H.E. Hoenig, B. Roas, and M. Leghissa for valuable discussions. This work was supported by the Bundesminister für Forschung und Technologie and by the Bayerische Forschungsförderung "Hochtemperatursupraleitung" (FORSUPRA).

- ¹R. Kleiner, F. Steinmeyer, G. Kunkel, and P. Müller, Phys. Rev. Lett. **68**, 2394 (1992).
- ²M. Tachiki and S. Takahashi, Solid State Commun. **72**, 1083 (1989).
- ³B. Roas, L. Schultz, and G. Saemann-Ischenko, Phys. Rev. Lett. **64**, 479 (1990).
- ⁴Y. Iye, T. Terashima, and Y. Bando, Physica C **184**, 362 (1991).
- ⁵P.H. Kes, J. Aarts, V.M. Vinikur, and C.J. van der Beck, Phys. Rev. Lett. **64**, 1063 (1990).
- ⁶P. Schmitt, P. Kummeth, L. Schultz, and G. Saemann-Ischenko, Phys. Rev. Lett. **67**, 267 (1991).
- ⁷J.R. Clem, Phys. Rev. B **43**, 7837 (1991).
- ⁸R. Busch, G. Ries, H. Werthner, G. Kreiselmeyer, and G. Saemann-Ischenko, Phys. Rev. Lett. **69**, 522 (1992).
- ⁹B. Roas, B. Hensel, S. Henke, S. Klaumünzer, B. Kabius, W. Watanabe, G. Saemann-Ischenko, L. Schultz, and K. Urban, Europhys. Lett. **11**, 669 (1990).
- ¹⁰L. Civale, A.D. Marwick, T.K. Worthington, M.A. Kirk, J.R. Thompson, L. Krusin-Elbaum, J.R. Clem, and F. Holtzberg, Phys. Rev. Lett. **67**, 648 (1991).
- ¹¹W. Gerhäuser, G. Ries, H.W. Neumüller, W. Schmidt, O. Eibel, G. Saemann-Ischenko, and S. Klaumünzer, Phys. Rev. Lett. **68**, 879 (1992).
- ¹²V. Hardy, D. Groult, J. Provost, and B. Raveaux, Physica C **190**, 289 (1992).
- ¹³J.R. Thompson, Y.R. Sun, H.R. Kerchner, D.K. Christen, B.C. Sales, B.C. Chakoumakos, A.D. Marwick, L. Civale, and J.O. Thomson, Appl. Phys. Lett. **60**, 2306 (1992).
- ¹⁴Th. Schuster, M.R. Koblischka, H. Kuhn, H. Kronmüller, M. Leghissa, W. Gerhäuser, G. Saemann-Ischenko, H.W. Neumüller, and S. Klaumünzer, Phys. Rev. B **46**, 8496 (1992).
- ¹⁵H. Watanabe, B. Kabius, K. Urban, B. Roas, S. Klaumünzer, and G. Saemann-Ischenko, Physica C **179**, 75 (1991).
- ¹⁶V. Hardy, D. Groult, M. Herrieu, J. Provost, and B. Raveau, Nucl. Instrum. Methods B **54**, 472 (1991).
- ¹⁷J. Dengler, G. Errmann, N. Kaner, G. Ritter, B. Hensel, M. Kraus, G. Kreiselmeyer, G. Saemann-Ischenko, S. Klaumünzer, and B. Roas, Hyperfine Interact. **70**, 921 (1992).
- ¹⁸J.M. Triscone, Ø. Fischer, O. Brunner, L. Antognazza, A.D. Kent, and M.G. Karkin, Phys. Rev. Lett. **64**, 804 (1990); D.H. Lowndes, D.P. Norton, and J.D. Budai, Phys. Rev. Lett. **65**, 1160 (1990); Q. Li, X.X. Xi, X.D. Wu, A. Inam, S. Vadlamannati, W.L. McLean, T. Vankatesan, R. Ramesh, D.M. Hwang, J.A. Marinez, and L. Nazar, Phys. Rev. Lett. **64**, 3086 (1990); G. Jakob, P. Przyslupski, C. Stölzel, C. Tomé-Rosa, A. Walkenhorst, M. Schmitt, and H. Adrian, Appl. Phys. Lett. **59**, 1627 (1991).
- ¹⁹B. Roas, L. Schultz, and G. Endres, Appl. Phys. Lett. **53**, 1557 (1988).
- ²⁰B. Holzapfel, B. Roas, L. Schultz, P. Bauer, and G. Saemann-Ischenko, Appl. Phys. Lett. **61**, 3178 (1992).
- ²¹B. Hensel, B. Roas, S. Henke, R. Hopfengärtner, M. Lippert, J.P. Ströbel, M. Vildić, G. Saemann-Ischenko, and S. Klaumünzer, Phys. Rev. B **42**, 4135 (1990).
- ²²G. Jakob, T. Hahn, C. Stölzel, C. Tomé-Rosa, and H. Adrian, Europhys. Lett. **19**, 135 (1992).
- ²³E.H. Brandt, Phys. Rev. Lett. **69**, 1105 (1992).